

Supplemental Materials

Hypomorphic variants of SEL1L-HRD1 ER-associated degradation are associated with neurodevelopmental disorders

Huilun Helen Wang^{1,2,17}, Lianguang Leo Lin^{1,2,17}, Zexin Jason Li^{1,3,17}, Xiaoqiong Wei^{1,2}, Omar Askander^{4,14}, Gerarda Cappuccio^{5,6,15}, Mais O. Hashem⁷, Laurence Hubert^{8,9}, Arnold Munnich⁸, Mashael Alqahtani⁷, Qi Pang¹⁰, Margit Burmeister¹¹, You Lu^{2,16}, Karine Poirier⁸, Claude Besmond⁸, Shengyi Sun^{12*}, Nicola Brunetti-Pierri^{5,6,13*}, Fowzan S. Alkuraya^{7*}, Ling Qi^{1,2,3,18*}

¹⁷These authors contributed equally to this work

* Correspondence: xvr2hm@virginia.edu (L.Q.); falkuraya@kfshrc.edu.sa; brunetti@tigem.it; bjk5fz@virginia.edu (S.S.)

Contents:

- Methods
- Supplemental Tables 1-2
- Supplemental Figures 1-6
- Supplemental Videos 1-3

METHODS

EXPERIMENTAL MODEL AND SUBJECT DETAILS

Genetic analysis

SEL1L: NM_005065:exon17:c.1754G>A:p.G585D

The patient was suspected of genetic disorders but received a negative Clinical Exome Sequencing (CES) report (no likely causal variant for the indication of the test was identified). Reanalysis of the negative clinical exome data of the patient was acquired as previously described (1). In brief, the venous blood samples were collected for genomic DNA extraction. Whole exome sequencing (WES) was performed using a TruSeq Exome Enrichment kit (Illumina Inc; San Diego, CA, USA) for exome capture, an Illumina Exome Enrichment protocol for library preparation, and an Illumina HiSeq 2000 Sequencer (Illumina Inc; San Diego, CA, USA) for sequencing. Sequence alignment, indexing of the reference genome (hg19), variant calling, and annotation were mapped and detected by Burrows-Wheeler Aligner (BWA, a software package for aligning sequencing reads against a large reference genome) and Sequence Alignment/Map Tools (SAMtools, a suite of programs for interacting with and post-processing short DNA sequence read in SAM format, which is a generic format for storing large nucleotide sequence alignments, <http://www.htslib.org/>), respectively. From the CES result, no pathogenic variants in OMIM were found to explain his phenotype, while during reanalysis, a homozygous variant in SEL1L (NM_005065:exon17:c.1754G>A:p.G585D) was highlighted as a potential candidate because the variant was absent in gnomAD and local databases and was consistently predicted to be deleterious by multiple *in silico* prediction tools, including BayesDel_addAF, Combined Annotation Dependent Depletion (CADD), DEOGEN2, FATHMM-MKL, LIST-S2, Mendelian Clinically Applicable Pathogenicity (M-CAP), MutationAssessor, MutationTaster, Polyphen2-HVAR, PrimateAI and Sorting Intolerant From Tolerant (SIFT).

SEL1L: NM_005065:exon16:c.1583T>G:p.M528R

This study is an ongoing collaboration between French and Moroccan hospitals. Blood samples and informed consent (from the patients' parents) of all family members were obtained according to the guidelines of local IRBs (APHP-Délégation Interrégionale à la Recherche Clinique). This study's protocol was conformed to the ethical guidelines of the 1975 Declaration of Helsinki as reflected in *a priori* approval by the institution's human research committee (Comité de Protection des Personnes). The whole blood samples were collected for genomic DNA extraction. WES was performed on patients 2 and 3 from 3 µg genomic DNA using an optimized Twist Human Core Exome kit (Twist Bioscience Inc; San Francisco, CA, USA) for

library preparation and an Illumina NovaSeq 6000 (Illumina Inc; San Diego, CA, USA) for sequencing. Sequence reads were aligned to the human genome (hg19) using BWA software. Downstream processing was carried out with the Genome analysis toolkit (GATK, a tool for identifying single nucleotide polymorphisms and indels in sequencing data, <https://gatk.broadinstitute.org/hc/en-us>), SAMtools, and Picard Tools (<http://picard.sourceforge.net/>). Single-nucleotide variants and indels were subsequently called by the SAMtools suite (mpileup, bcftools, vcfutil). All calls with a read coverage $\leq 5\times$ and a Phred-scaled SNP quality of ≤ 20 were filtered out. Substitution and variation calls were made with the SAMtools pipeline (mpileup). Variants were annotated with an in-house bioinformatics platform pipeline based on the Ensembl database (release 67). Selected variants were confirmed by direct sequencing using BigDye dideoxy terminator chemistry and an ABI3130xl genetic DNA analyzer (Applied Biosystems) after PCR using genomic DNA from the patients and other family members.

HRD1: NM_172230:exon12:c.1193C>T;p.P398L

The proband was excluded from previous genetic tests and enrolled in the Telethon Undiagnosed Disease Program for exome sequencing. Genomic DNA was collected from the proband and both parents. The WES was performed by using Agilent Sureselect Clinical Research Exome (Agilent, Technologies, Santa Clara, CA) for library preparation and an Illumina NextSeq 500 sequencing system (Illumina, San Diego, CA) for sequencing. A custom pipeline based on the Burrows-Wheeler Alignment tool, the Genome Analysis Toolkit, and ANNOVAR (2) was used to call, annotate, filter, and prioritize variants.

Protein structure modeling

The individual structure models of human SEL1L, HRD1, OS9, and DERLIN1 were downloaded from AlphaFold2 database (<https://alphafold.ebi.ac.uk/>) (3). The complex structure was constructed using TM-align (4) by superposing the predicted human SEL1L, HRD1, OS9, and DERLIN1 structures to the CryoEM structure of the yeast Hrd3p-Hrd1p-Der1p protein complex (PDB ID: 6VJZ) and Hrd3p-Yos9 complex (PDB ID: 6VK3). All the structure images of human SEL1L residues 171-723, HRD1 1-334, OS9 33-655 and DERLIN1 1-213 were rendered by PyMOL (version 2.3.2). To analyze the evolutionary conservation of each residue, a position-specific scoring matrix (PSSM) was generated for each protein from a PSI-BLAST search of the target protein through the NCBI NR database (5, 6). IUPred2A (7) was used to predict the disordered regions of HRD1 protein. The regions where IUPred2A score >0.5 are considered as

disordered regions. Sequence alignments were generated by ClustalW program. The evolutionary conservation of amino acids between the protein and its homologues was calculated using ConSurf (8).

(Non-)reducing SDS-PAGE

HEK293T cells transfected with proAVP(G57S)-HA plasmid were snap-frozen in liquid nitrogen and whole cell lysates were prepared in the NP-40 lysis buffer supplemented with protease and phosphatase inhibitors and 10 mM N-ethylmaleimide. Lysates were incubated on ice for 30 min and centrifuged at 16,000×g for 10 min. Supernatants were collected and analyzed for protein concentration using the Bio-Rad Protein Assay Dye (Bio-Rad). For reducing SDS-PAGE analysis, lysates were denatured at 95°C for 5 min in the 5x SDS sample buffer. For non-reducing SDS-PAGE analysis, the lysates were prepared in 5x non-denaturing sample buffer (250 mM Tris-HCl pH 6.8, 1% sodium dodecyl sulfate, 0.05% Bromophenol blue, 50% glycerol) and incubated at 37°C for 1 hour. The samples were loaded into a 4%-12% gradient or 6% gel for separation.

RNA preparation and RT-PCR

Total RNA was extracted from tissues and cells using TRI Reagent and BCP phase separation reagent (Molecular Research Center, TR 118). RT-PCR primer sequences are (m, mouse; h, human):

hSEL1L F: AAACCAGCTTTGACCGCCAT R: GTCATAGGTTGTAGCACACCAC

hHRD1 F: CCTGCGTAACATCCACACAC R: TCTGAGCTAGGGATGCTGGT

hL32 F: AGTTCCTGGTCCACAACGTC R: TTGGGGTTGGTGA CTCTGAT

hXBP1: F: 5'-GAATGAAGTGAGGCCAGTGG-3' R: ACTGGGTCCTTCTGGGTAGA

REFERENCES

1. Shamseldin HE, Maddirevula S, Faqeih E, Ibrahim N, Hashem M, Shaheen R, and Alkuraya FS. Increasing the sensitivity of clinical exome sequencing through improved filtration strategy. *Genet Med.* 2017;19(5):593-8.
2. Wang K, Li M, and Hakonarson H. ANNOVAR: functional annotation of genetic variants from high-throughput sequencing data. *Nucleic Acids Res.* 2010;38(16):e164.

3. Jumper J, Evans R, Pritzel A, Green T, Figurnov M, Ronneberger O, et al. Highly accurate protein structure prediction with AlphaFold. *Nature*. 2021;596(7873):583-9.
4. Zhang Y, and Skolnick J. TM-align: a protein structure alignment algorithm based on the TM-score. *Nucleic Acids Res*. 2005;33(7):2302-9.
5. Altschul SF, Madden TL, Schaffer AA, Zhang J, Zhang Z, Miller W, and Lipman DJ. Gapped BLAST and PSI-BLAST: a new generation of protein database search programs. *Nucleic Acids Res*. 1997;25(17):3389-402.
6. Sayers EW, Bolton EE, Brister JR, Canese K, Chan J, Comeau DC, et al. Database resources of the national center for biotechnology information. *Nucleic Acids Res*. 2022;50(D1):D20-D6.
7. Meszaros B, Erdos G, and Dosztanyi Z. IUPred2A: context-dependent prediction of protein disorder as a function of redox state and protein binding. *Nucleic Acids Res*. 2018;46(W1):W329-W37.
8. Ashkenazy H, Abadi S, Martz E, Chay O, Mayrose I, Pupko T, and Ben-Tal N. ConSurf 2016: an improved methodology to estimate and visualize evolutionary conservation in macromolecules. *Nucleic Acids Res*. 2016;44(W1):W344-50.

SUPPLEMENTAL TABLE

Supplemental Table 1. Candidate variants identified in probands and the prediction of deleteriousness.

Probands	Gene	Full gene name	Variants	Zygoty	Chr	pLI score [†]	CADD	PolyPhen-2 HVAR	SIFT
Patient 1 (Saudi Arabian)	<i>SEL1L</i>	Suppressor of lin12-like	c.1754G>A; p.G585D	Homozygous*	14	0.98	+	+	+
	<i>RAB17</i>	Ras-associated protein rab17	Splice site mutation	Homozygous	2	0.07	-	N/A	N/A
	<i>VWA5B2</i>	von Willebrand factor A containing 5B2 domain	c.1475C>G; p.S492C	Homozygous	3	0	+	+	+
	<i>SLC25A53</i>	Solute carrier family 25, member 53	c.347T>A; p.H116L	Homozygous	X	0.06	-	-	-
	<i>ERI3</i>	Prion protein-interacting protein	c.950C>T;p.A317V	Compound heterozygous	1	0	+	+	-
			Splice site mutation				N/A	N/A	N/A
	<i>FRYL</i>	FRY like transcription coactivator	c.7490C>G;p.T2497R	Heterozygous	4	1	+	+	-
	<i>ADH5</i>	Alcohol dehydrogenase 5, chi polypeptide	c.938_943del; p.313_315del	Compound heterozygous	4	0	N/A	N/A	N/A
			Splice site mutation				N/A	N/A	N/A
	<i>FGB</i>	Fibrinogen, b beta polypeptide	Splice site mutation	Heterozygous	4	0.57	-	N/A	N/A
<i>SYNE3</i>	Spectrin repeat-containing nuclear envelope protein 3	Splice site mutation	Heterozygous	14	0	-	N/A	N/A	
<i>SKA3</i>	Spindle- and kinetochore-associated complex, subunit	Splice site mutation	Heterozygous	12	0	N/A	N/A	N/A	
Patient 2-5 (Moroccan)	<i>SEL1L</i>	Suppressor of lin12-like	c.1583T>G; p.M528R	Homozygous*	14	0.98	+	+	-

Patient 6 (Italian)	<i>HRD1</i>	Synovial apoptosis inhibitor, SYVN1	c.1193C>T; p.P398L	Homozygous*	11	1	+	-	-
	<i>MS4A12</i>	Membrane-spanning 4-domains, subfamily a, member 12	c.277G>A; p.V93M	Homozygous	11	0	+	+	+
	<i>PPP1R32</i>	Protein phosphatase 1, regulatory subunit 3	c.473A>G; p.Q158R	Homozygous	11	0	+	+	-
	<i>IBTK</i>	Inhibitor of bruton agammaglobulinemia tyrosine kinase	c.2795delC; p.P932fs	De novo	6	0	N/A	N/A	N/A
	<i>LSP1</i>	Lymphocyte-specific protein	Splice site mutation	De novo	11	0	-	N/A	N/A
	<i>KNL1</i>	Kinetochores scaffold	c.5974G>T; p.A1992S	Compound heterozygous	15	0.78	-	-	+
			Splice site mutation				N/A	N/A	N/A
	<i>OBSCN</i>	Obscurin	c.2309G>A; p.R770Q;	Compound heterozygous	1	0	-	-	N/A
c.17125G>A; p.V5709M;			+				+	+	
c.20303G>A; p.R6768Q;			-				-	N/A	
c.23419G>A; p.V7807I			-				-	N/A	
Splice site mutation			N/A				N/A	N/A	

Chr, Chromosome; pLI, probability of being loss-of-function intolerant; CADD, Combined Annotation Dependent Depletion; PolyPhen-2-HVAR, Polymorphism Phenotyping v2, HumVar-trained model; SIFT, Sorting Intolerant From Tolerant; +, CADD score >20, or probably damaging (Polyphen-2), or damaging (SIFT); -, CADD score ≤20, or benign (Polyphen-2), or tolerated (SIFT); N/A: Not Applicable; Splice site mutation: a genetic mutation in the mRNA splicing site; * Confirmed to be segregated in the parents; † Based on gnomAD v2.1.1.

Supplemental Table 2. Clinical features of patients with *SEL1L* and *HRD1* variants.

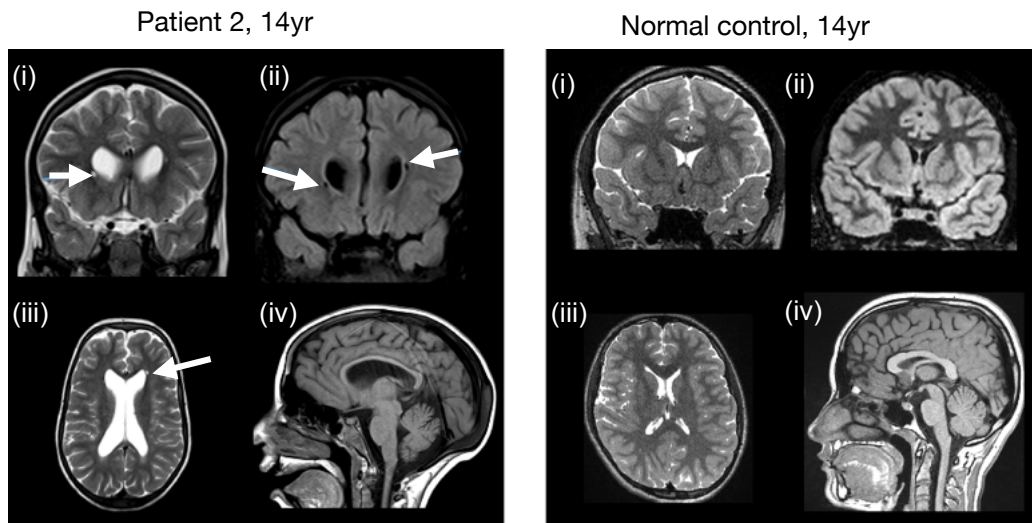
	Patient 1 (Saudi Arabia)	Patient 2 (Morocco)	Patient 3 (Morocco)	Patient 4 (Morocco)	Patient 5 (Morocco)	Patient 6 (Italy)
Date of birth (MM/YYYY)	Oct-2009	Jun-2005	Dec-2007	Feb-2011	Oct-2017	Nov-2001
Time of last visit (MM/YYYY)	May-2022	Jun-2022	Jun-2022	Jun-2022	Jun-2022	Jun-2022
Sex	M	F	M	M	M	F
Ethnicity	Middle Eastern (Arab)	North African (Moroccan)				European
Consanguinity	+	+				-
Coding variants	SEL1L p.Gly585Glu	SEL1L p.Met528Arg				HRD1 p.Pro398Leu
Zygoty	Homozygous					
Intellectual disability	Moderate to severe, IQ35	Severe, no speech, few words				Severe, no words
Hypotonia/ Ataxia	Brisk deep tendon reflexes, wide-based gait with hands held on the side to support the balance. No dystonia. Cerebellar involvement is negative. The symptom did not progress since 08/2022.	Severe spastic and ataxic gait, falls, wide-based gait, pes cavus and equinus, mild dystonia, paraparesia with pyramidal signs of lower limbs, with brisk, diffused tendon reflexes and clonus, pyramidal extension of the first toe, Babinski signs		Progressive ataxia, wide-based gait, stepping gate, brisk reflexes, Babinski sign but no pes cavus/equinus at this stage	Milder Progressive ataxia, wide-based gait, stepping gate, neither frank spasticity nor brisk reflexes, no pes cavus/equinus at this stage	Mild clumsy gait at early age, resolved now. The symptom did not progress.
Developmental milestones delay	Sat at 2 years of age, walked at 5, uttered mama/dada at 6 and is not yet toilet trained. Currently, he can only make limited two-word sentences	No speech	No speech	No speech	No speech	No speech

	and cannot count to 3.					
Short stature	+ (-3.9 SD)	+	+	+	+	+ (<5 ^o percentile)
Underweight	+ (-3.9 SD)	+	+	+	+	+ (<5 ^o percentile)
Microcephaly	+ (-4.2SD)	- (54cm, 39 ^o percentile)	- (53cm, 10 ^o percentile)	+ (50cm, 1 ^o percentile)	+ (47cm, <1 ^o percentile)	+ (<5 ^o percentile)
Seizures	Total of 3 seizures at 8 years of age.	One single generalized tonicoclonic seizure (3 min) at 2 years old	One single generalized tonicoclonic seizure (30 min) at 10 years old	No epileptic seizure to date	No epileptic seizure to date	Drug-resistant seizures
Dysmorphisms	Downslanting palpebral fissures, overbite, joint hyperlaxity, pectus excavatum and shawl scrotum	Varus equus, scoliosis and arched palate	ND	Scoliosis	ND	Orbital hypertelorism and flat nasal bridge
Brain imaging abnormalities	-	Cortical-subcortical atrophy	ND	ND	ND	Abnormal signal in the globus pallidum and substantia nigra
EEG abnormalities	-	Generalized discharges of polyspikes and slow waves. Hyperventilation not done. Stable Awake EEG showed theta activity in	ND	ND	ND	-

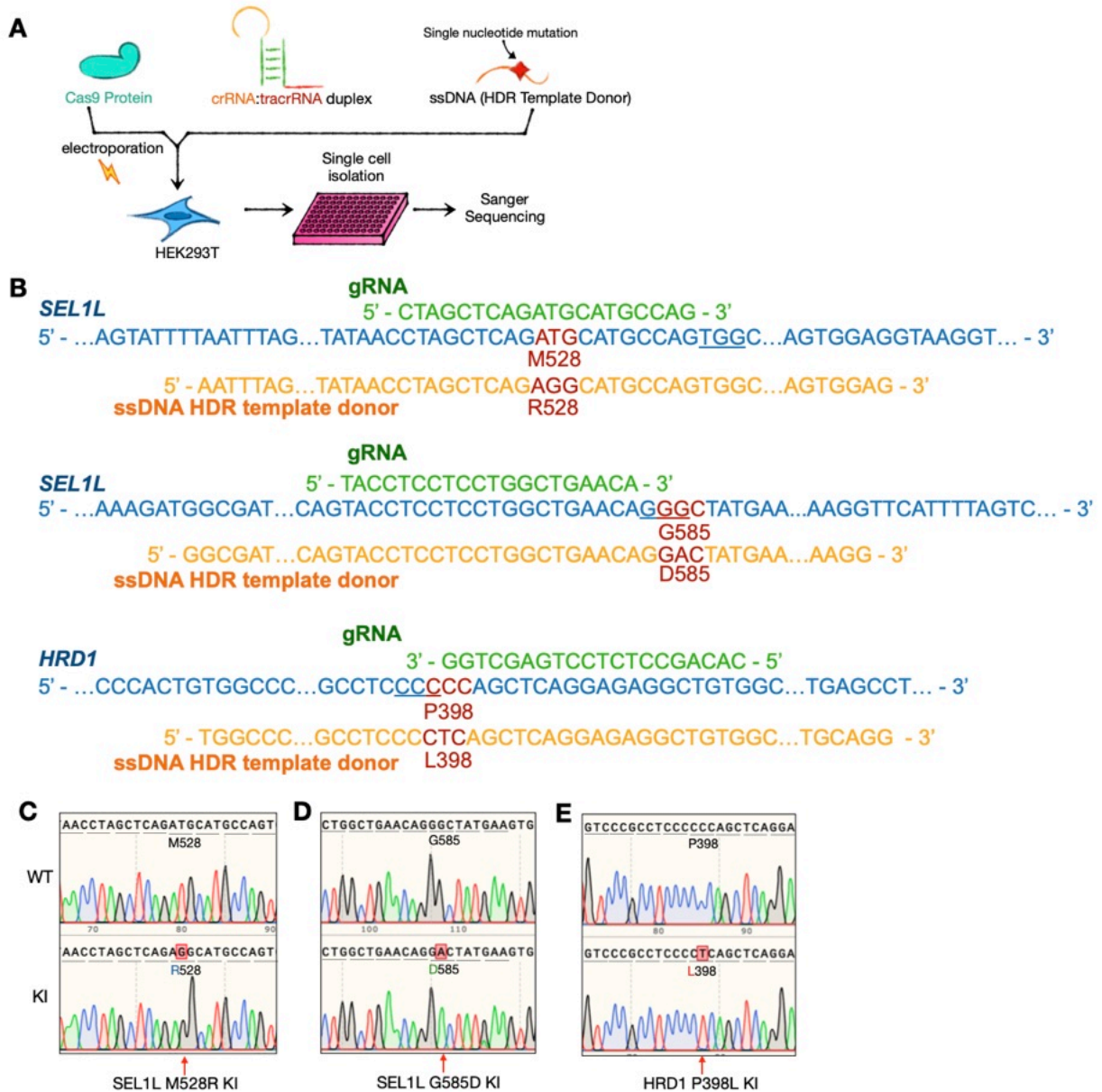
		parieto-occipital areas.				
Blood tests	Mild hypochromic microcytic anemia and iron deficiency	Vitamin D deficiency and an infection at the time of tests on 06/22.	ND	ND	ND	-
Eye symptom	Cataract	unilateral maculopathy, pallor of temporal poles, keratopathy, severe corneal dystrophy	ND	ND	ND	-
Immunity	Medical history is notable for frequent chest infections and hypothyroidism although no evidence of immunodeficiency					No clinical evidence of immune dysfunction

M, Male; F, Female; SD, standard deviation; ND, not determined.
+, showing abnormality; -, no significant findings.

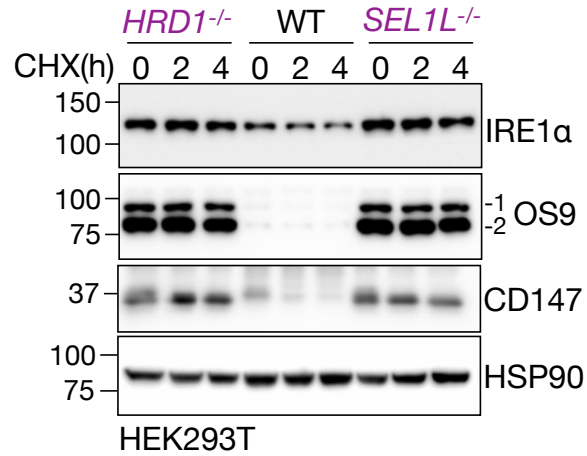
SUPPLEMENTAL FIGURES AND FIGURE LEGENDS



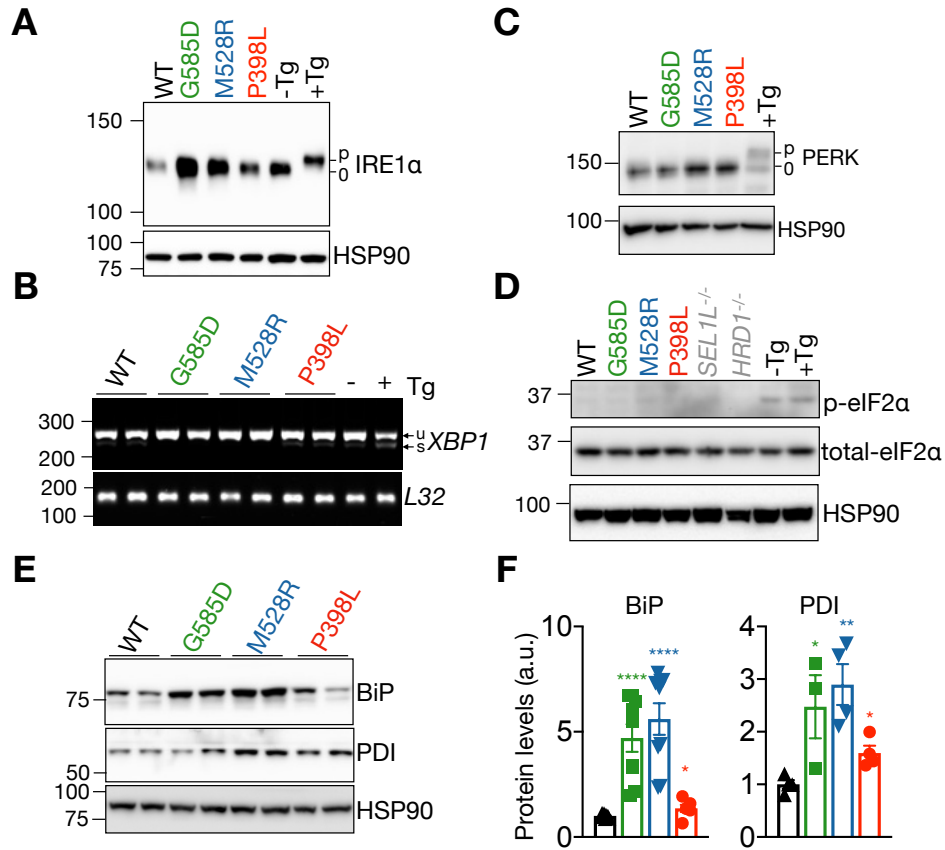
Supplemental Figure 1. MR imaging of Patient 2 and a healthy control. Brain MRIs of Patient 2 at 14 years of age and an age-matched healthy control. Note small cavities in the frontal periventricular area (arrows) with non-specific ventricular dilatation on coronal T2 (i), coronal FLAIR (ii) and axial T2 (iii) weighted images. On sagittal plane (iv), note the thin corpus callosum with no anomalies of basal ganglia or at the infra tentorial level.



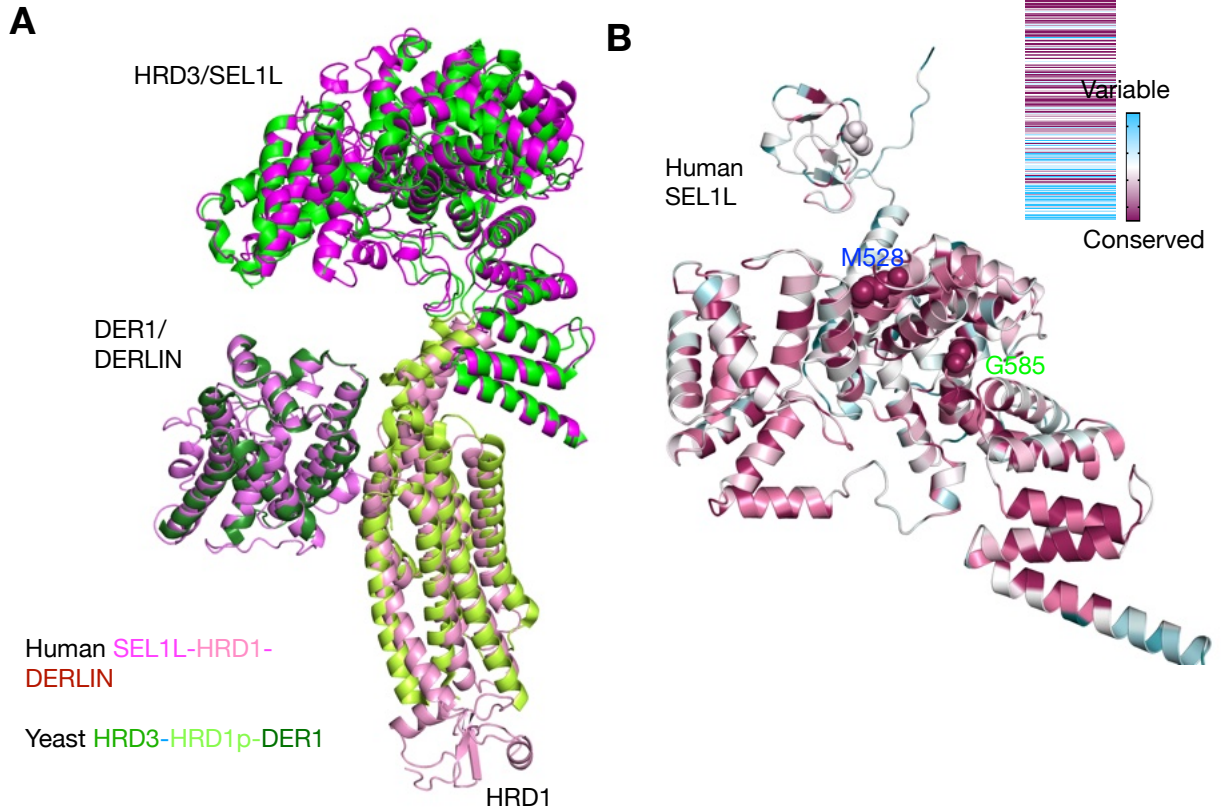
Supplemental Figure 2. Generation of knock-in (KI) HEK293T cells carrying the variants via CRISPR-Cas9. (A) Schematic diagram of the generation of *SEL1L* M528R, G585D and *HRD1* P398L knock-in (KI) HEK293T cells using the CRISPR/Ca9 technology. (B) gRNA and ssDNA HDR template donor designs for each variant. PAM sites are underlined. (C-E) Sanger sequencing confirmation of *SEL1L* M528R (C), G585D (D) and *HRD1* P398L KI HEK293T (E). The shaded red box and arrow indicate the mutations.



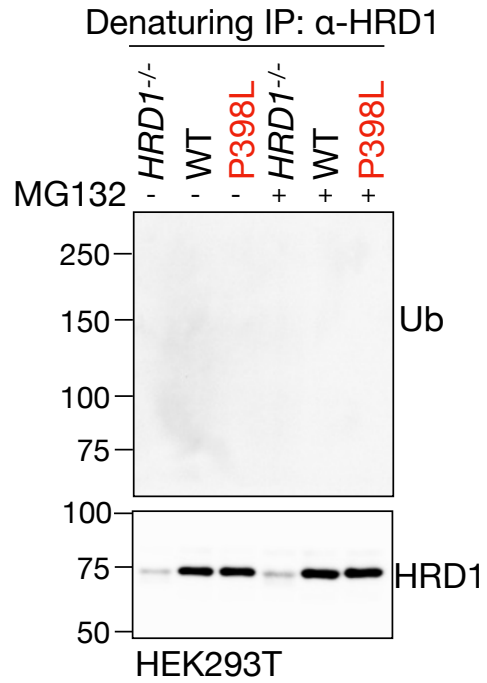
Supplemental Figure 3. Loss of SEL1L-HRD1 ERAD causes substrate accumulation. Western blot analysis of known ERAD endogenous substrates IRE1α, OS9 and CD147 in SEL1L and HRD1 KO HEK293T cells treated with cycloheximide (CHX) for the indicated times. Quantitation shown in Figure 3D.



Supplemental Figure 4. *SEL1L* or *HRD1* variants are not associated with an overt UPR. (A-D) Phos-tag gel analysis of IRE1α phosphorylation (A), RT-PCR of *XBP1* mRNA splicing (B), Western blot analysis of PERK and eIF2α phosphorylation (C-D) in WT and KI HEK293T cells. WT HEK293T cells treated with 100nM thapsigargin (+Tg) or DMSO (-Tg) for 4 hr as controls. u, unspliced. s, spliced. p, phosphorylated. 0, unphosphorylated. The replicates shown in (B) are technical replicates. Experiments were repeated for three times independently for (A-D). (E-F) Western blot analysis of ER chaperones BiP and PDI in WT and various KI HEK293T cells with quantitation shown in (F). * $p < 0.05$, ** $p < 0.01$ and **** $p < 0.0001$ by two-tailed Student's *t*-test for comparison between WT and HRD1 P398L cells and one-way ANOVA followed by Dunnett's multiple comparisons test for the comparison between *SEL1L* variants and WT (F).



Supplemental Figure 5. Structural conservation of SEL1L-HRD1 ERAD protein complexes between human and yeast. (A) Structure alignment between human and yeast SEL1L-HRD1-
DERLIN complexes. **(B)** Predicated 3D structure of human SEL1L colored by ConSurf
conservation score.



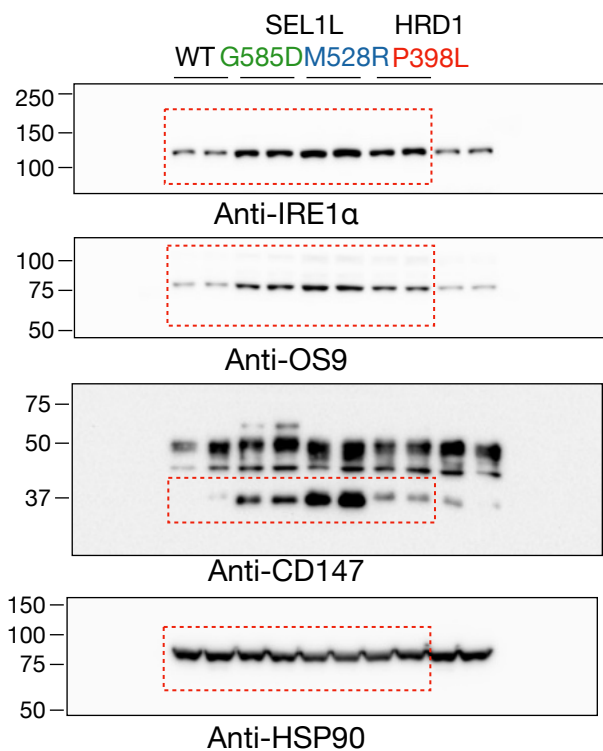
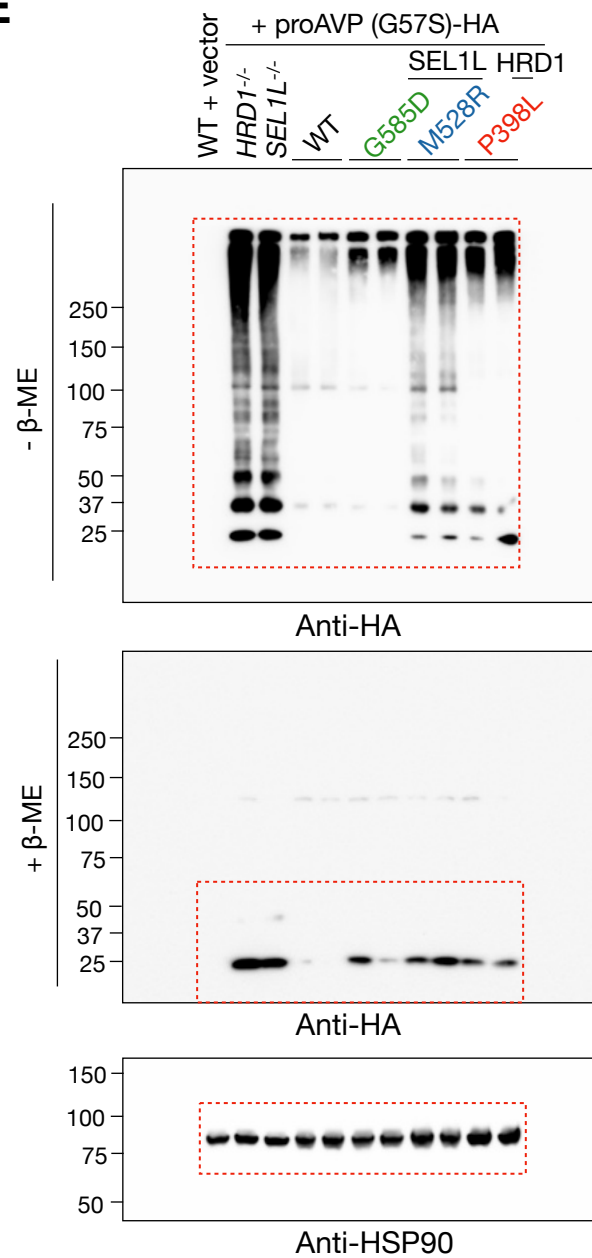
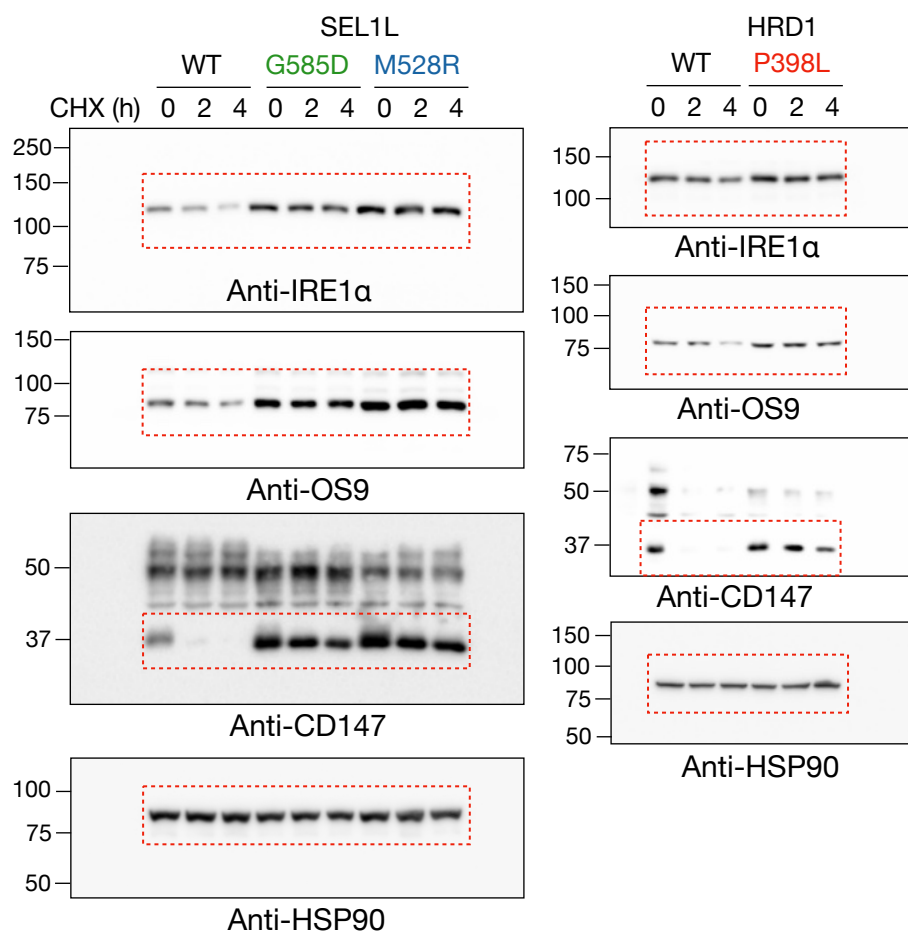
Supplemental Figure 6. Failure to detect ubiquitination of endogenous HRD1 protein. Western blot of ubiquitin following denaturing immunoprecipitation in WT, *HRD1*^{-/-} and HRD1 *P398L* KI HEK293T cells with or without treatment of MG132. Exposure time = 2000s.

SUPPLEMENTAL VIDEOS

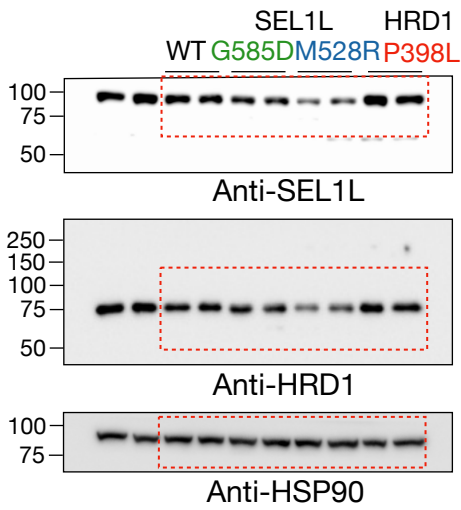
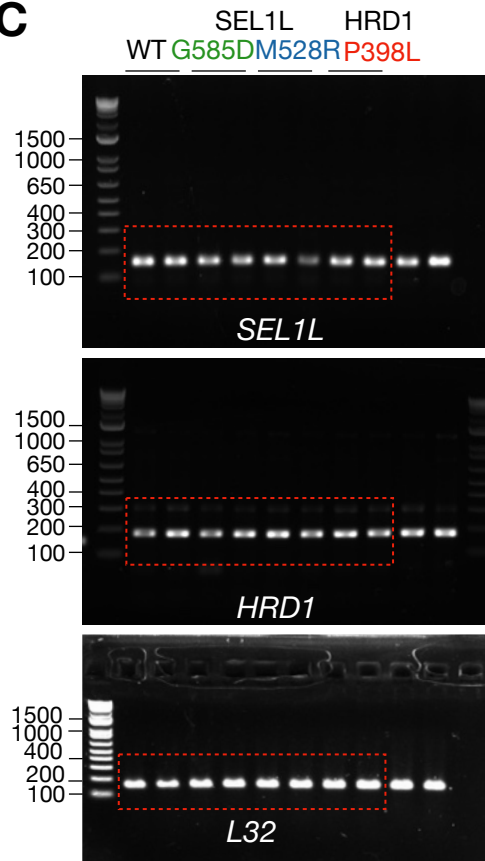
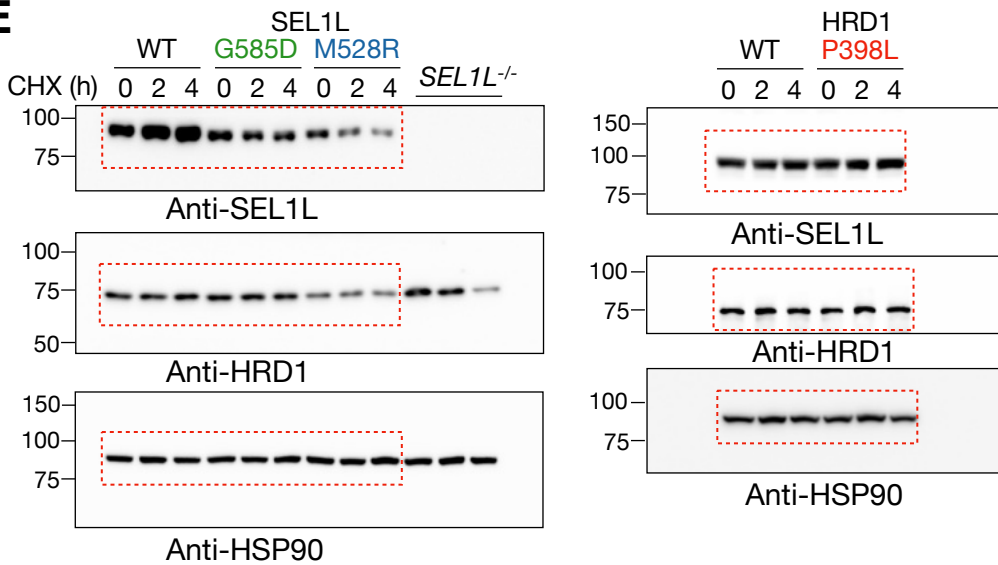
Supplemental Video 1. Patient 1 carrying *SEL1L* p.G585D variant at 13 years of age. Video shows the patient walking with clumsy gait and clenching fists stiffly besides the body.

Supplemental Video 2. Patient 2 carrying *SEL1L* p.M528R variant at 17 years of age. Video shows the patient walking with wide-based gait, balancing with hand support, hypotonia and ataxia.

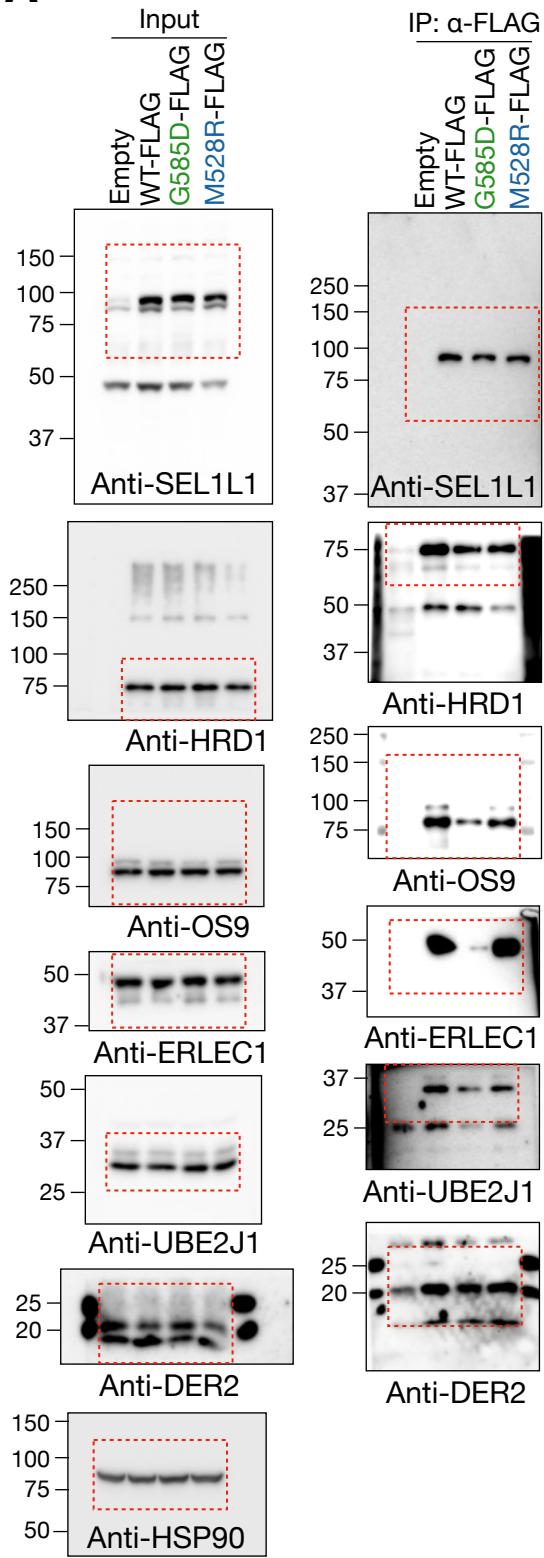
Supplemental Video 3. Patient 6 carrying *HRD1* p.P398L variant at 21 years of age. Video shows the patient walking and climbing the stairs. The patient also shows stereotypies with repetitive, purposeless hand movements.

A**E****C**

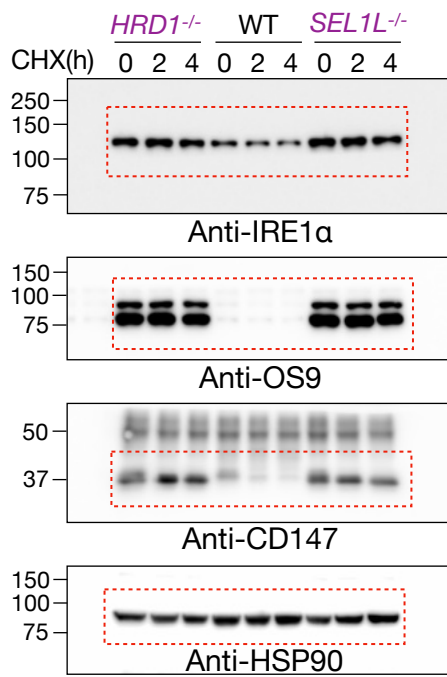
Full unedited gels for
Figure 3, A, C and E

A**C****E**

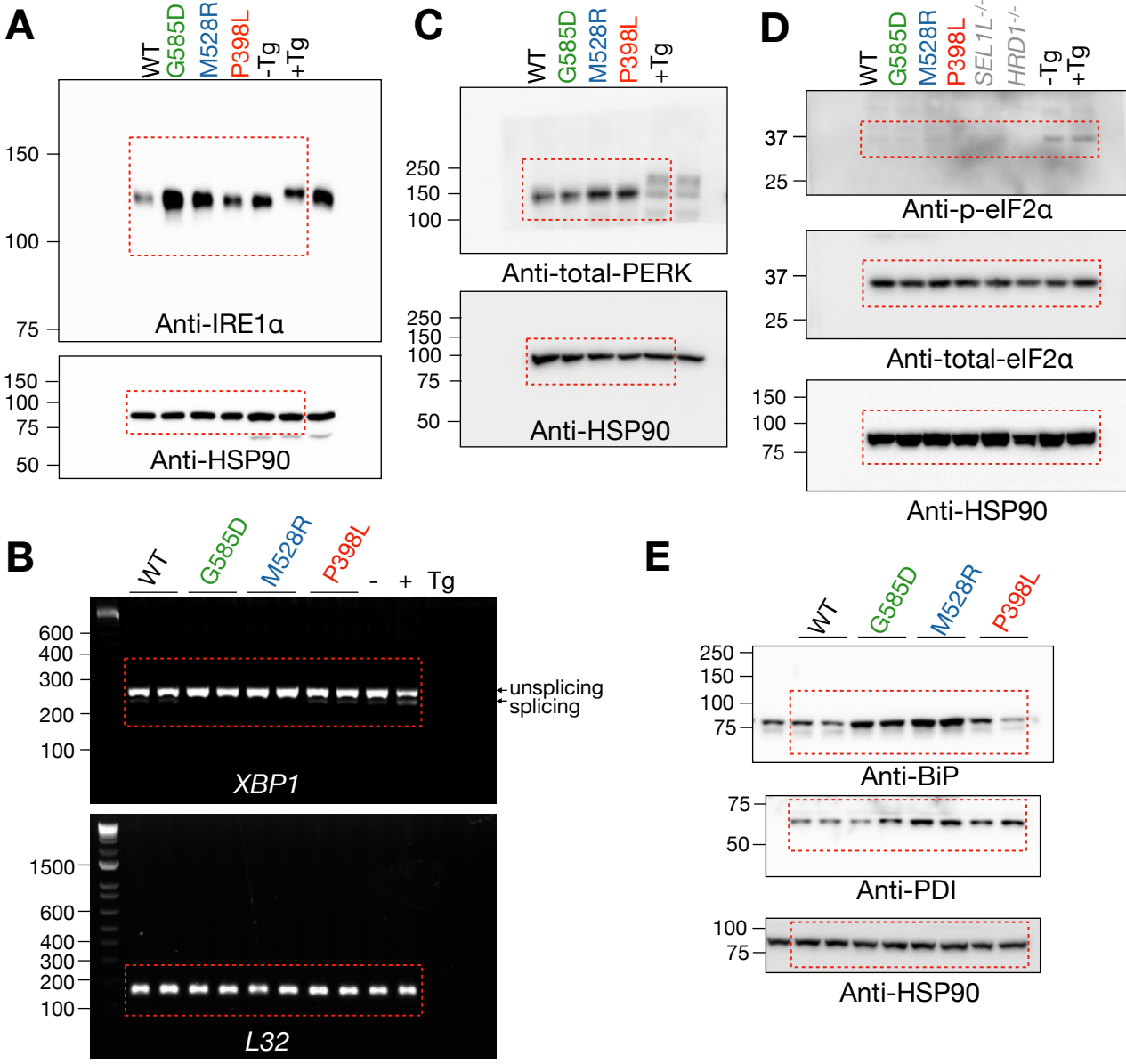
Full unedited gels for Figure 5, A, C and E

A

Full unedited gels for Figure 6A

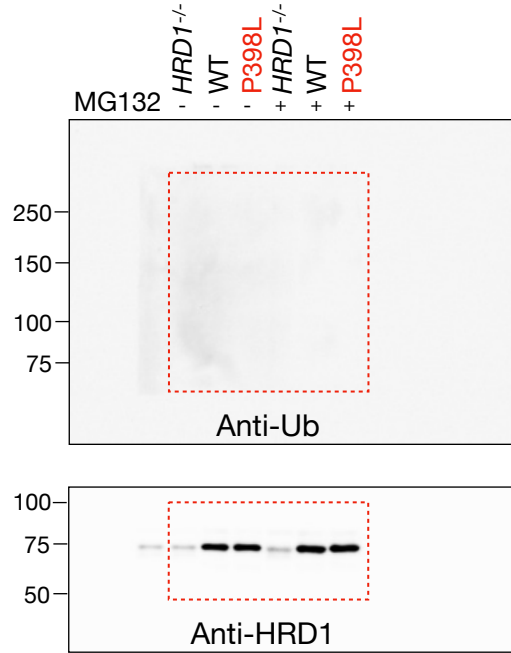


Full unedited gels for
Supplemental Figure 3



Full unedited gels for Supplemental Figure 4, A-E

Denaturing IP: α -HRD1



Full unedited gels for
Supplemental Figure 6